UNIVERSITY OF LEEDS



---

**Article:**
Cao, K and Lesnic, D (2018) Reconstruction of the space-dependent perfusion coefficient from final time or time-average temperature measurements. Journal of Computational and Applied Mathematics, 337. pp. 150-165. ISSN 0377-0427

https://doi.org/10.1016/j.cam.2018.01.010

---

# Reconstruction of the space-dependent perfusion coefficient from final time or time-average temperature measurements

K. Cao, D. Lesnic*

*Department of Applied Mathematics, University of Leeds, Leeds, LS2 9JT, United Kingdom*

**Abstract**

Knowledge of the blood perfusion in biomedicine is of crucial importance in applications related to hypothermia. In this paper, we consider the inverse bio-heat transfer nonlinear problem to determine the space-dependent perfusion coefficient from final time or time-average temperature measurements, which are themselves space-dependent quantities. In other applications this coefficient multiplying the temperature function represents a reaction rate. Uniqueness of solution holds but continuous dependence on the input data is violated. The problem is reformulated as a least-squares minimization whose gradient is obtained by solving the sensitivity and adjoint problems. The newly obtained gradient formula is used in the conjugate gradient method (CGM). This is the first time that the CGM is applied to solve the inverse problems under investigation. For exact data, we investigate the convergence of the iterative CGM. We also test that the iterative algorithm is semi-convergent under noisy data by stopping the iteration using the discrepancy principle criterion to produce a stable solution. Furthermore, because the search step size is computed using an optimization scheme at each iteration the CGM is very efficient. Three examples are investigated to verify the accuracy and stability of the numerical method.

*Keywords:* Inverse problem; Heat transfer; Conjugate gradient method; Perfusion coefficient

## 1. Introduction

Blood perfusion is defined as the blood volume flow exchange per volume of tissue, which refers to the local, multidirectional blood flow through the capillaries and intracellular space of living tissue, and its measurements can determine the success or failure of skin grafts and any related healing, [1, 2]. Unlike the bulk flow through the larger vessels, blood perfusion is considered to be a directionless quantity at the macroscopic level due to the convoluted nature of the pathways through which it moves. Capillary and intracellular space blood flow is responsible for providing the oxygen and nutrients required by cells of the body, and removing waste products to maintain life processes. Prior to this study, several parameter estimation least-squares techniques were utilized for the determination of blood perfusion using non-invasive measurements from minimally surface probe, [1, 3, 4, 5].

In the next two subsections, we briefly review some of the representative works and results on the identification of the space-dependent perfusion coefficient. Identifications of time- or temperature-dependent perfusion coefficient have been considered elsewhere, [6, 7].

*Corresponding author

*Email addresses:* mmkc@leeds.ac.uk (K. Cao), amt5ld@maths.leeds.ac.uk (D. Lesnic)

### *1.1. Review of some theoretical works*

For reliability, in general, mathematical modelling should be formulated such that the resulting inverse problem cannot have more than one solution, i.e. the solution is unique if it exists. It is not sufficient to state the desirables if the observations are not properly chosen. Therefore, uniqueness studies and results are of crucial importance prior to undertaking any numerical solution.

The uniqueness of the space-dependent perfusion coefficient in Hölder spaces for the bio-heat equation with homogeneous Neumann boundary condition, initial and final data was established in [8]. In [9], the uniqueness in the same Hölder space of functions with the same data, but with zero initial condition and non-homogeneous Dirichlet boundary condition was proved. In [10], existence and uniqueness for the space-dependent perfusion coefficient in Hölder spaces were established for the bio-heat equation with non-homogeneous initial and Dirichlet boundary conditions and two distinct types of over-determination: the final temperature data and the temperature at a fixed point in the interior of the relevant space region for all values of time.

In [11, 12], the existence and uniqueness of the space-dependent perfusion coefficient in Sobolev spaces for the bio-heat equation with non-homogeneous Dirichlet boundary condition and time-average temperature measurement were established. Finally, the uniqueness of the space-dependent perfusion coefficient in Sobolev spaces from homogeneous initial and boundary conditions with inhomogeneous source and final or time-average temperature data was established in [13]. There are these latter inverse formulations that are proposed to be investigated numerically in this paper.

### *1.2. Review of some numerical works*

In [14], the space-dependent perfusion coefficient was determined in the one-dimensional bio-heat equation with homogeneous Neumann boundary condition, and initial and final observations, as in the inverse problem formulated and theoretically investigated in [8]. The unknown coefficient was reconstructed by minimizing the first-order nonlinear Tikhonov regularization functional. Numerical results were obtained using the finite-difference method (FDM) and an elliptic bilateral variational inequality. In [15], the same inverse problem as in [14] was discussed from discrete final temperature observations. On the basis of an interpolation technique, a new way was found to reconstruct the coefficient by minimizing the same Tikhonov regularization functional. In [16], the space-dependent perfusion coefficient was determined in the bio-heat equation with homogeneous Dirichlet boundary condition and final temperature measurement. A different weighted objective gradient functional was minimized to identify the coefficient. The coefficient was obtained numerically by applying the Armijo algorithm combined with the finite element method (FEM).

Finally, in [17], the space-dependent perfusion coefficient was determined in the one-dimensional bio-heat equation with non-homogeneous Dirichlet boundary condition and heat flux or time-average temperature measurement. The first-order Tikhonov regularization functional was minimized using the NAG routine E04FCF together with the FDM to obtain the numerical solution for the unknown coefficient.

In this paper, the determination of the space-dependent perfusion coefficient from final time or time-average temperature measurements in the bio-heat equation with initial and boundary conditions is obtained by minimizing the nonlinear least-squares objective functional. The Fréchlet gradient of the objective functional is obtained. In order to obtain a stable numerical solution, the CGM algorithm regularized by the discrepancy principle, [18, 19], is developed apparently for the first time for the inverse problems under investigation. Three examples are presented, and the numerical results obtained using the CGM and the FDM show that the CGM algorithm regularized by the discrepancy principle is efficient and stable for identifying the space-dependent perfusion

coefficient. It is also found that the specification of the time-average temperature contains more information than the instant final time temperature measurement.

The plan of the paper is as follows. The mathematical formulations of the coefficient identification problems under investigation are presented are section 2. The numerical CGM algorithm based on the sensitivity and adjoint problems is presented in section 3. Numerical results are presented and discussed in section 4 and finally, section 5 highlights the conclusions of the work.

## 2. Mathematical formulation

The most common heat transfer model in tissue is obtained by balancing the accumulation of energy with the diffusion, heat transfer due to the blood flow through the capillary network and heat generation due to cell metabolism, to result in the well-known Pennes' bio-heat equation, [20]. We consider therefore the bio-heat transfer problem in a bounded domain $\Omega \subset \mathbb{R}^N$, $N$ is usually 1, 2 or 3, with sufficiently smooth boundary $\partial\Omega$, representing the tissue, over the time interval $t \in (0, t_f)$, where $t_f > 0$ is a final time of interest, given by the bio-heat equation

$$\mathrm{C}\frac{\partial T}{\partial t}(x,t) = \nabla \cdot (k(x)\nabla T(x,t)) - q(x)T(x,t) + S(x,t), \quad (x,t) \in Q := \Omega \times (0,t_f), \tag{1}$$

subject to the Dirichlet boundary condition

$$T(x,t) = \mu(x,t), \quad (x,t) \in \partial\Omega \times (0,t_f), \tag{2}$$

and the initial condition

$$T(x,0) = T_0(x), \quad x \in \overline{\Omega}, \tag{3}$$

where $T(x,t)$ is the unknown tissue temperature, $q(x) \geq 0$ is the unknown space-dependent perfusion coefficient, $k = (k_{ij}(x))_{i,j=\overline{1,N}}$ denotes the known thermal conductivity of the tissue satisfying

$$k_{ij} = k_{ji} \in C^1(\Omega), \quad 0 < \nu_1 \leq \sum_{i,j=1}^{N} k_{ij}(x)\xi_i\xi_j \leq \nu_2, \quad \forall x \in \Omega, \forall \xi \in \mathbb{R}^N \text{with } |\xi| = 1, \tag{4}$$

for some given positive constants $\nu_1$ and $\nu_2$, $\mathrm{C} > 0$ is the heat capacity of the tissue assumed to be constant and taken, for simplicity, equal to unity, $S(x,t)$ is the given metabolic heat source, $\mu$ is the given Dirichlet boundary temperature and $T_0$ is the given initial temperature at $t = 0$. The equation (4) states the physical property that the thermal conductivity tensor is symmetric and positive definite. Neumann heat flux or Robin convective boundary conditions can also be considered instead of (2). Of course, because the coefficient $q(x)$ in (1) is unknown we need additional information, and in this study we supply either the final temperature at $t = t_f$, namely,

$$e(x) = T(x,t_f), \quad x \in \Omega, \tag{5}$$

or the time-average temperature measurement

$$E(x) = \int_0^{t_f} \omega(t)T(x,t)dt, \quad x \in \Omega, \tag{6}$$

where $\omega(t) \in L_1(0,t_f)$ is some given weight function, and $e(x)$ and $E(x)$ are given data which may be subjected to noise due to measurement errors. Compatibility conditions between (2), (5) and (6) require that

$$e(x) = \mu(x,t_f), \quad x \in \partial\Omega, \tag{7}$$

and

$$E(x) = \int_0^{t_f} \omega(t)\mu(x,t)dt, \quad x \in \partial\Omega, \tag{8}$$

respectively. In (1), the blood perfusion coefficient $q$ is the product between the heat capacity of the blood $C_b$ and the blood perfusion rate $\omega_b$, and the arterial blood temperature has been assumed to be uniform and taken, for simplicity, equal to zero.

There are two inverse problems, namely (1)–(5) and (1)–(3), (6), termed IP1 and IP2, respectively, which may be formulated for the determination of the space-dependent perfusion coefficient $q(x) \geq 0$ together with the temperature $T(x,t)$. These two inverse problems possess in common the fundamental property that both the input data, $e(x)$ or $E(x)$, and output data, $q(x)$, are space-dependent. A different inverse Cauchy-type problem in which, instead of (5) or (6), we have a time-dependent boundary measurement of the heat flux,

$$k(x)\nabla T(x,t)\cdot n(x) = j(x,t), \quad (x,t) \in \partial\Omega \times (0,t_f) \tag{9}$$

where $n$ is the outward unit normal to the boundary $\partial\Omega$, is not investigated herein, but we mention [21, 22]. The existence and uniqueness of the classical solution in Hölder spaces of the IP1 was established in [10]. For the IP2, existence of a generalized solution was established in [11] and [12], whilst [13] established uniqueness of generalized solutions in Sobolev spaces for both IP1 and IP2. In particular, it is useful to state in subsection 2.2 these uniqueness results.

*2.1. Preliminaries and notations*

In this section we give some notation on functional spaces from [23, 24].

The space $L_2(\Omega)$ consists of all square-integrable functions over $\Omega$, equipped with the norm

$$\|u\|_{L_2(\Omega)} = \left\{ \int_\Omega |u(x)|^2 dx \right\}^{1/2}. \tag{10}$$

The space $L_\infty(\Omega)$ comprises all essentially bounded functions in $\Omega$, having the norm

$$\|u\|_{L_\infty(\Omega)} = \operatorname*{ess\,sup}_{x\in\Omega} |u(x)| = \inf\{M \geq 0; |u(x)| \leq M, \text{a.e. } x \in \Omega\}. \tag{11}$$

The space $C^1(\Omega)$ is the set of all continuous functions in $\Omega$ having continuous first-order derivatives in $\Omega$, equipped with the norm

$$\|u\|_{C^1(\Omega)} = \sum_{|\alpha|\leq 1} \sup_\Omega |D^\alpha u| \tag{12}$$

where $\alpha = (\alpha_1, \ldots, \alpha_N)$ is a multi-index, $\alpha_i \geq 0$, $i = \overline{1,N}$, $|\alpha| = \sum_{i=1}^N \alpha_i$ and $D^\alpha u = \frac{\partial^{|\alpha|} u}{\partial x_1^{\alpha_1} \cdots \partial x_N^{\alpha_N}}$.

We assume that $\partial\Omega$ is smooth enough, e.g. of class $C^{2+h}$ for some $h \in (0,1)$, i.e., each point of $\partial\Omega$ has a neighbourhood in which $\partial\Omega$ is the graph of a function $x_N = f(x_1, \cdots, x_{N-1})$ of class

$C^{2+h}$ consisting of functions which themselves and all derivatives up to the second-order are Hölder continuous with exponent $h$.

The Hölder space $C^h(\overline{\Omega})$ is the set of all continuous functions in $\overline{\Omega}$ which are Hölder continuous with exponent $h$, equipped with the norm

$$\|u\|_{C^h(\overline{\Omega})} = \sup_{\overline{\Omega}} |u| + \sup_{x,x' \in \overline{\Omega}} \frac{|u(x) - u(x')|}{|x - x'|^h}. \tag{13}$$

We also denote the non-negative cones

$$C^h_+(\overline{\Omega}) = \{u \in C^h(\overline{\Omega}) | u \geq 0\}, \quad L^+_\infty(\Omega) = \{u \in L_\infty(\Omega) | u \geq 0\}. \tag{14}$$

The Sobolev space $W_2^1(\Omega)$ is defined by

$$W_2^1(\Omega) = \{u \in L_2(\Omega) : D^\alpha u \in L_2(\Omega) \text{ with } |\alpha| \leq 1\} \tag{15}$$

equipped with the norm

$$\|u\|_{W_2^1(\Omega)} = \left\{ \sum_{|\alpha| \leq 1} \|D^\alpha u\|^2_{L_2(\Omega)} \right\}^{1/2}. \tag{16}$$

The Sobolev space $W_2^{2,1}(Q)$ is defined as a Banach space of all functions $u$ belonging to $L_2(Q)$ along with their first and second-order space derivatives and the first-order time derivative. The norm in this space is defined by

$$\|u\|_{W_2^{2,1}(Q)} = \left\{ \sum_{|\alpha| \leq 2} \|D^\alpha u\|^2_{L_2(Q)} + \|\partial u/\partial t\|^2_{L_2(Q)} \right\}^{1/2}. \tag{17}$$

The anisotropic Hölder space $C^{2+h,1+h/2}(\overline{Q})$ for $h \in (0,1)$ is a Banach space of all functions $u$ in $Q$ that are continuous on $\overline{Q}$ and that possess space derivatives up to and including the second order and time derivatives of the first order, which are Hölder continuous on $x$ and $t$ with exponents $h$ and $h/2$, respectively. The norm on the space is defined by

$$\begin{aligned}
\|u\|_{C^{2+h,1+h/2}(\overline{Q})} &= \sum_{|\alpha| \leq 2} \sup_{\overline{Q}} |D^\alpha u| + \sup_{\overline{Q}} |\partial u/\partial t| \\
&+ \sum_{|\alpha|=2} \sup_{(x,t),(x',t) \in \overline{Q}} \frac{|D^\alpha u(x,t) - D^\alpha u(x',t)|}{|x - x'|^h} + \sup_{(x,t),(x,t') \in \overline{Q}} \frac{|\partial u(x,t)/\partial t - \partial u(x,t')/\partial t|}{|t - t'|^{h/2}} \\
&+ \sum_{|\alpha|=2} \sup_{(x,t),(x,t') \in \overline{Q}} \frac{|D^\alpha u(x,t) - D^\alpha u(x,t')|}{|t - t'|^{h/2}} + \sup_{(x,t),(x',t) \in \overline{Q}} \frac{|\partial u(x,t)/\partial t - \partial u(x',t)/\partial t|}{|x - x'|^h}.
\end{aligned} \tag{18}$$

Throughout the paper the symbol $\Delta$ denotes an increment of the quantity to which is attached. For the Laplacian operator we use the symbol $\nabla^2$.

*2.2. Results*

First, we state the existence and uniqueness of the solution for the direct problem (1)–(3) when all the coeficients and boundary and initial conditions are known functions (see [23], pp. 341).

**Theorem 1.** *Suppose that $k$ satisfies (4), $q \in L_\infty(\Omega)$, $S \in L_2(Q)$, $T_0 \in W_2^1(\Omega)$ and $\mu \equiv 0$. Then the direct problem (1)–(3) satisfying the compatibility condition $T_0|_{\partial\Omega} = 0$ has a unique solution $T \in W_2^{2,1}(Q)$ which satisfies the estimate*

$$\|T\|_{W_2^{2,1}(Q)} \le c\left(\|S\|_{L_2(Q)} + \|T_0\|_{W_2^1(\Omega)}\right). \tag{19}$$

*The constant $c = c(t_f)$ remains bounded for finite values of $t_f$.*

Next, we state the uniqueness results for the IP1 and IP2.

**Theorem 2** ([13])**.** *Let $\Omega$ be a bounded simply connected domain in $\mathbb{R}^N$, $N \ge 1$ with boundary $\partial\Omega \in C^2$. Suppose that $T_0 = \mu \equiv 0$, $0 \le S \in L_2(Q)$, $0 \le S_t \in L_2(Q)$, $0 \le \omega \in L_2(0, t_f)$. Then:*

*(i) if $e > 0$ in $\Omega$ (or $E > 0$ in $\Omega$) the solution of the IP1 (or IP2) is unique in the class of functions $(T, q) \in W_2^{2,1}(Q) \times L_\infty^+(\Omega)$;*

*(ii) alternatively, the same uniqueness result holds if $S(\cdot, t_f) \not\equiv 0$ for IP1, or $\int_0^{t_f} \omega(t)S(\cdot, t)dt \not\equiv 0$ for IP2.*

Note that in [9], the author proved the uniqueness of solution to IP1 in the Hölder space $C^{2+h,1+h/2}(\overline{Q}) \times C_+^h(\overline{\Omega})$, provided that $S \equiv 0$, $T_0 \equiv 0$, $\mu \ge 0$ and $0 \not\equiv \partial\mu/\partial t \ge 0$, and compatibility conditions up to the second order are satisfied. Also, in [8], the author proved the uniqueness of solution to the inverse problem (1), (3), (5) and (9) in $C^{2+h,1+h/2}(\overline{Q}) \times C_+^h(\overline{\Omega})$ provided that $k = I_N =$ identity tensor, $S \equiv 0$, $j \equiv 0$, $C^{1+h}(\Omega) \ni T_0 \ge 0$, $\nabla T_0|_{\partial\Omega} = \mathbf{0}$ and $e \in C^h(\Omega)$.

*2.3. Mathematical analysis*

Let $T(x, t; q)$ denote the solution of the direct problem, that is, the temperature corresponding to a particular value of the unknown function $q(x)$. The quasi-solution of the IP1 or IP2 is obtained such that the following least-squares objective functionals are minimized:

$$J_1[q] = \frac{1}{2}\|T(\cdot, t_f; q) - e(\cdot)\|_{L_2(\Omega)}^2 \tag{20}$$

or

$$J_2[q] = \frac{1}{2}\left\|\int_0^{t_f} \omega(t)T(\cdot, t; q)dt - E(\cdot)\right\|_{L_2(\Omega)}^2 \tag{21}$$

over the admissible set $L_\infty^+(\Omega)$, subject to $T \in W_2^{2,1}(Q)$ satisfying the direct problem (1)–(3).

We then solve the minimization problem (20) with the final measured data $e \in L_2(\Omega)$ for IP1, and (21) with the time-average measured data $E \in L_2(\Omega)$ for IP2.

**Lemma 3.** *The mapping $q \mapsto T(q)$ is Lipschitz continuous from $L_\infty^+(\Omega)$ to $W_2^{2,1}(Q)$, i.e., for any $q$, $q + \Delta q \in L_\infty^+(\Omega)$ and the corresponding $T(q)$, $T(q + \Delta q) \in W_2^{2,1}(Q)$, there holds*

$$\|T(q + \Delta q) - T(q)\|_{W_2^{2,1}(Q)} \le c\|\Delta q\|_{L_\infty(\Omega)}. \tag{22}$$

*Proof.* Denote $\Delta T = T(q + \Delta q) - T(q)$, then $\Delta T$ satisfies the problem

$$\frac{\partial(\Delta T)}{\partial t} = \nabla \cdot [k\nabla(\Delta T)] - q\Delta T - \Delta q T(q + \Delta q), \quad (x, t) \in Q, \tag{23}$$

$$\Delta T(x, t) = 0, \quad (x, t) \in \partial\Omega \times (0, t_f), \tag{24}$$

$$\Delta T(x, 0) = 0, \quad x \in \overline{\Omega}. \tag{25}$$

Using (19) in Theorem 1 to the problem (23)–(25), we obtain

$$\|\Delta T\|_{W_2^{2,1}(Q)} \le c\|\Delta q T\|_{L_2(Q)} \le c\|\Delta q\|_{L_\infty(\Omega)}\|T\|_{L_2(Q)} \le c\|\Delta q\|_{L_\infty(\Omega)}\|T\|_{W_2^{2,1}(Q)}.$$

Since $\|T\|_{W_2^{2,1}(Q)}$ is bounded by the estimate (19), this concludes the proof of the lemma. □

Note that the problem (23)–(25) is the sensitivity problem used in the CGM iterative algorithm later, and is the same for both IP1 and IP2.

**Lemma 4.** *The mapping $q \mapsto T(q)$ from $L_\infty^+(\Omega)$ to $W_2^{2,1}(Q)$ is Fréchet differentiable in the sense that for any $\Delta q \in L_\infty(\Omega)$ such that $q + \Delta q \in L_\infty^+(\Omega)$ there exists a bounded linear operator $\mathcal{U} : L_\infty(\Omega) \mapsto W_2^{2,1}(Q)$ such that*

$$\lim_{\|\Delta q\|_{L_\infty(\Omega)} \to 0} \frac{\|T(q+\Delta q) - T(q) - \mathcal{U}\Delta q\|_{W_2^{2,1}(Q)}}{\|\Delta q\|_{L_\infty(\Omega)}} = 0. \tag{26}$$

*Proof.* Consider the problem

$$\frac{\partial u}{\partial t} = \nabla \cdot (k\nabla u) - qu - \Delta q T(q), \quad (x,t) \in Q, \tag{27}$$

$$u(x,t) = 0, \quad (x,t) \in \partial\Omega \times (0,t_f), \tag{28}$$

$$u(x,0) = 0, \quad x \in \overline{\Omega}, \tag{29}$$

where $\Delta q \in L_\infty(\Omega)$ such that $q + \Delta q \in L_\infty^+(\Omega)$. Theorem 1 shows that there exists a unique solution $u(x,t) \in W_2^{2,1}(Q)$ of (27)–(29), and the map $\Delta q \mapsto u$ from $L_\infty(\Omega)$ to $W_2^{2,1}(Q)$ defines a bounded linear operator $\mathcal{U}$ by (19).

Denote $w = T(q+\Delta q) - T(q) - \mathcal{U}\Delta q = \Delta T - u$, where $\Delta T$ satisfies the problem (23)–(25) and rewrite (23) as

$$\frac{\partial(\Delta T)}{\partial t} = \nabla \cdot [k\nabla(\Delta T)] - q\Delta T - \Delta q(\Delta T + T(q)), \quad (x,t) \in Q. \tag{30}$$

Thus, $w$ satisfies the problem

$$\frac{\partial w}{\partial t} = \nabla \cdot (k\nabla w) - qw - \Delta q \Delta T, \quad (x,t) \in Q, \tag{31}$$

$$w(x,t) = 0, \quad (x,t) \in \partial\Omega \times (0,t_f), \tag{32}$$

$$w(x,0) = 0, \quad x \in \overline{\Omega}. \tag{33}$$

By applying (19), we obtain

$$\|w\|_{W_2^{2,1}(Q)} \le c\|\Delta q \Delta T\|_{L_2(Q)} \le c\|\Delta q\|_{L_\infty(\Omega)}\|\Delta T\|_{L_2(Q)} \le c\|\Delta q\|_{L_\infty(\Omega)}\|\Delta T\|_{W_2^{2,1}(Q)},$$

and using (22), we obtain that $\|w\|_{W_2^{2,1}(Q)} \le c\|\Delta q\|^2_{L_\infty(\Omega)}$. Therefore, (26) is proved. □

**Theorem 5.** *The function $J_1$ is Fréchlet differentiable and its gradient is*

$$J_1'[q] = -\int_0^{t_f} T(x,t)\lambda_1(x,t)dt, \tag{34}$$

*where $\lambda_1(x,t)$ satisfies the following adjoint problem:*

$$\frac{\partial \lambda_1}{\partial t} = -\nabla \cdot (k\nabla \lambda_1) + q\lambda_1 - 2(T(x,t_f;q) - e(x))\delta(t-t_f), \quad (x,t) \in Q, \tag{35}$$

$$\lambda_1(x,t) = 0, \quad (x,t) \in \partial\Omega \times (0,t_f), \tag{36}$$

$$\lambda_1(x,t_f) = 0, \quad x \in \overline{\Omega}, \tag{37}$$

*and $\delta$ is the Dirac delta function.*

*Proof.* Taking any $\Delta q \in L_\infty(\Omega)$ such that $q + \Delta q \in L_\infty^+(\Omega)$, we have

$$\begin{aligned} J_1[q+\Delta q] - J_1[q] =& \frac{1}{2}\int_\Omega (T(x,t_f;q+\Delta q) - e(x))^2 dx - \frac{1}{2}\int_\Omega (T(x,t_f;q) - e(x))^2 dx \\ =& \frac{1}{2}\|\Delta T(\cdot,t_f)\|^2_{L_2(\Omega)} + \int_\Omega \Delta T(x,t_f)(T(x,t_f;q) - e(x))dx. \end{aligned}$$

Now we introduce $\lambda_1(x,t) \in W_2^{2,1}(Q)$, being the solution of the final boundary value problem (35)–(37). Using (23)–(25) and integration by parts, we have

$$\begin{aligned} & J_1[q+\Delta q] - J_1[q] \\ &= \int_Q 2\Delta T(x,t)(T(x,t_f;q) - e(x))\delta(t-t_f)dxdt + \frac{1}{2}\|\Delta T(\cdot,t_f)\|^2_{L_2(\Omega)} \\ &= \int_Q \Delta T \left( -\frac{\partial \lambda_1}{\partial t} - \nabla \cdot (k\nabla\lambda_1) + q\lambda_1 \right) dxdt + \frac{1}{2}\|\Delta T(\cdot,t_f)\|^2_{L_2(\Omega)} \\ &= \int_Q \lambda_1 \left\{ \frac{\partial \Delta T}{\partial t} - \nabla \cdot (k\nabla(\Delta T)) + q\Delta T \right\} dxdt - \int_\Omega \Delta T \lambda_1|_0^{t_f} dx + \frac{1}{2}\|\Delta T(\cdot,t_f)\|^2_{L_2(\Omega)} \\ &\quad + \int_0^{t_f}\int_{\partial\Omega} (k\lambda_1 \nabla(\Delta T) - k\Delta T(\nabla\lambda_1))\, dsdt \\ &= -\int_Q \Delta q T(q+\Delta q)\lambda_1 dxdt + \frac{1}{2}\|\Delta T(\cdot,t_f)\|^2_{L_2(\Omega)} \\ &= -\int_Q \Delta q \Delta T \lambda_1 dxdt - \int_Q \Delta q T \lambda_1 dxdt + \frac{1}{2}\|\Delta T(\cdot,t_f)\|^2_{L_2(\Omega)}. \end{aligned} \tag{38}$$

Since $\Delta T$ is the solution of problem (23)–(25), in virtue of Lemma 3, we have $\|\Delta T(\cdot,t_f)\|^2_{L_2(\Omega)} \le \|\Delta T\|^2_{W_2^{2,1}(Q)} \le c\|\Delta q\|^2_{L_\infty(\Omega)}$, and

$$\left| \int_Q \Delta q \Delta T \lambda_1 dxdt \right| \le \|\Delta q\|_{L_\infty(\Omega)} \|\Delta T\|_{L_2(Q)} \|\lambda_1\|_{L_2(Q)} \le c\|\Delta q\|^2_{L_\infty(\Omega)} \|\lambda_1\|_{L_2(Q)},$$

thus

$$J_1[q+\Delta q] - J_1[q] = -\int_Q \Delta q T \lambda_1 dxdt + o(\|\Delta q\|_{L_\infty(\Omega)}),$$

which means that the function $J_1$ is Fréchlet differentiable, and its gradient is given by (34). The theorem is proved. □

Note that the gradient $J_1'[q]$ given by (34) and the adjoint problem (35)–(37) are for the inverse problem IP1. The adjoint problem is different from the standard initial value problems in that the final time condition at time $t = t_f$ is specified instead of the customary initial condition. However, the problem can be transformed into an initial value problem by the transformation of the time variable $\bar{t} = t_f - t$.

**Remark 6.** *For the functional $J_2[q]$ of the inverse problem IP2, similar properties can be obtained, i.e., $J_2[q]$ is Fréchlet differentiable and its gradient is*

$$J_2'[q] = -\int_0^{t_f} T(x,t)\lambda_2(x,t)dt, \tag{39}$$

*where $\lambda_2(x,t)$ satisfies the following adjoint problem:*

$$\frac{\partial \lambda_2}{\partial t} = -\nabla\cdot(k\nabla\lambda_2) + q\lambda_2 - \omega(t)\left(\int_0^{t_f}\omega(\tau)T(x,\tau;q)d\tau - E(x)\right), \quad (x,t)\in Q, \tag{40}$$

$$\lambda_2(x,t) = 0, \quad (x,t)\in\partial\Omega\times(0,t_f), \tag{41}$$

$$\lambda_2(x,t_f) = 0, \quad x\in\overline{\Omega}. \tag{42}$$

One can show, [25], that there exists a minimizer of (20) (or (21)).

## 3. Conjugate gradient method (CGM)

The following iterative process based on the CGM is now used for the estimation of $q(x)$ by minimizing the objective functional $J[q]$, where $J$ stands for $J_1$ or $J_2$:

$$q^{n+1}(x) = q^n(x) - \beta^n P^n(x), \quad n = 0,1,2,\cdots \tag{43}$$

where the subscript $n$ denotes the number of iterations, $q^0(x)$ is the initial guess for $q(x)$, $\beta^n$ is the step search size in passing from iteration $n$ to iteration $n+1$, and $P^n(x)$ is the direction of descent given by

$$P^0(x) = J'[q^0(x)], \quad P^n(x) = J'[q^n(x)] + \gamma^n P^{n-1}(x), \quad n = 1,2,\cdots \tag{44}$$

Different expressions are avalible for the conjugate coefficient $\gamma^n$, e.g., for the Fletcher–Reeves method [18, 26, 27]

$$\gamma^0 = 0, \quad \gamma^n = \frac{\|J'[q^n]\|^2_{L_2(\Omega)}}{\|J'[q^{n-1}]\|^2_{L_2(\Omega)}}, \quad n = 1,2,\cdots. \tag{45}$$

For the IP1, the search step size $\beta^n$ is found by minimizing

$$J_1[q^{n+1}] = \frac{1}{2}\int_\Omega \left[T(x,t_f;q^n - \beta^n P^n) - e(x)\right]^2 dx. \tag{46}$$

Setting $\Delta q^n = P^n$, the estimated temperature $T(x,t_f;q^n-\beta^n P^n)$ is linearised by a Taylor series expression in the form

$$T(x,t_f;q^n-\beta^n P^n) \approx T(x,t_f;q^n) - \beta^n P^n \frac{\partial T(x,t_f;q^n)}{\partial q^n} \approx T(x,t_f;q^n) - \beta^n \Delta T(x,t_f;q^n)$$

and $\Delta T(x,t_f;q^n)$ is the solution of the sensitivity problem (23)–(25) when $t=t_f$ by setting $\Delta q^n = P^n$. Then, we have

$$J_1[q^{n+1}] = \frac{1}{2}\int_\Omega \left[T(x,t_f;q^n) - \beta^n \Delta T(x,t_f;q^n) - e(x)\right]^2 dx.$$

Then, we calculate the derivative of $J_1[q^{n+1}]$ with respect to $\beta^n$ and get

$$\frac{\partial J_1}{\partial \beta^n} = -\int_\Omega \left[T(x,t_f;q^n) - \beta^n \Delta T(x,t_f;q^n) - e(x)\right] \Delta T(x,t_f;q^n) dx.$$

Next, we set $\frac{\partial J_1}{\partial \beta^n} = 0$, and we obtain the search step size $\beta^n$ for IP1, as follows:

$$\beta^n = \frac{\int_\Omega \left[T(x,t_f;q^n) - e(x)\right] \Delta T(x,t_f;q^n) dx}{\|\Delta T(\cdot,t_f;q^n)\|^2_{L_2(\Omega)}}. \tag{47}$$

We also can obtain the search step size $\beta^n$ for IP2 via a similar method. We have

$$\begin{aligned} J_2[q^{n+1}] =& \frac{1}{2}\int_\Omega \left[\int_0^{t_f} \omega(t) T(x,t;q^n - \beta^n P^n) dt - E(x)\right]^2 dx \\ =& \frac{1}{2}\int_\Omega \left[\int_0^{t_f} \omega(t) T(x,t;q^n) dt - \beta^n \int_0^{t_f} \omega(t) \Delta T(x,t;q^n) dt - E(x)\right]^2 dx. \end{aligned}$$

Then the derivative of $J_2[q^{n+1}]$ with respect to $\beta^n$ is

$$\frac{\partial J_2}{\partial \beta^n} = -\int_\Omega \left[\int_0^{t_f} \omega(t) T(x,t;q^n) dt - \beta^n \int_0^{t_f} \omega(t) \Delta T(x,t;q^n) dt - E_i\right] \int_0^{t_f} \omega(t) \Delta T(x,t;q^n) dt dx.$$

Again we set $\frac{\partial J_2}{\partial \beta^n} = 0$, and obtain

$$\beta^n = \frac{\int_\Omega \left(\int_0^{t_f} \omega(t) T(x,t;q^n) dt - E(x)\right) \int_0^{t_f} \omega(t) \Delta T(x,t;q^n) dt dx}{\|\omega(\cdot) \Delta T(\cdot,\cdot;q^n)\|^2_{L_2(Q)}}. \tag{48}$$

The iterative procedure given by equation (43) does not provide the CGM with the stabilization necessary for the minimization of the function (20) or (21) to be classified as well-posed because of the errors inherent in the measurements (5) or (6). However, the CGM may become well-posed if the discrepancy principle is used to stop the iterative procedure.

In the discrepancy principle, the iterative procedure is stopped when the following criterion satisfied:

$$J[q^n] \approx \frac{1}{2}\mu^2, \tag{49}$$

where

$$\mu = \|Y - Y^{exact}\|_{L_2(\Omega)}, \tag{50}$$

where $Y$ means the noisy measured data $e$ and $E$ for the inverse problems IP1 and IP2, respectively.

The steps of the CGM algorithm for IP1 (and similarly for IP2) are shown as follows:

1 Choose an initial guess $q^0(x)$ and set $n=0$.

2 Solve the direct problem (1)–(3) by applying a finite-difference scheme to compute $T(x,t;q^n)$ and $J_1[q^n]$ by equation (20).

3 Solve the adjoint problem (35)–(37) to compute the Lagrange multiplier $\lambda(x,t;q^n)$, and the gradient $J_1'[q^n]$ from the equation (34). Compute the conjugate coefficient $\gamma^n$, and the direction of descent $P^n(x)$.

4 Solve the sensitivity problem (23)–(25) to compute the sensitivity function $\Delta T(x,t;q^n)$ by taking $\Delta q^n(x) = P^n(x)$, and compute he search step size $\beta^n$ by (47).

5 Compute $q^{n+1}(x)$ by (43). In case $q^{n+1}(x)$ takes negative values replace it by $\max\{0, q^{n+1}(x)\}$ in order to enforce the physical constraint that the perfusion coefficient cannot be negative.

6 The stopping condition is:

If $J_1[q^n] \approx \frac{1}{2}\mu^2$ go to step 7.

Else set $n = n+1$ go to step 2.

7 End

## 4. Numerical results and discussions

We use the FDM, [28], based on the Crank-Nicolson method in one-dimension $N = 1$, or the alternating direction implicit (ADI) method in two-dimensions $N = 2$, to solve the direct, sensitivity and adjoint problems. Local or global meshless collocation procedures can also be employed, [29]. Note that in (35) the source term contains the Dirac delta function which is approximated by

$$\delta(t - t_f) \approx \frac{1}{a\sqrt{\pi}} e^{-(t-t_f)^2/a^2}, \tag{51}$$

where $a$ is a small positive constant taken as $a = 10^{-3}$. The Simpson's rule is used to deal with all the integrations in this paper.

We define the error at the iteration number $n$ for the perfusion coefficient $q(x)$ as

$$Err[q^n] = \|q - q^n\|_{L_2(\Omega)}. \tag{52}$$

The final temperature measurements $e$ for IP1 containing random errors are simulated by adding to $e^{exact}$ an error term generated from a normal distribution by MATLAB in the form:

$$e = e^{exact} + \text{random}('\text{Normal}', 0, \sigma, I, 1), \tag{53}$$

where $\sigma = \frac{p}{100} \times \max_{x\in\overline{\Omega}} |e^{exact}(x)|$ is the standard deviation and $p\%$ represents the percentage of noise. Similarly, the average temperature measurements $E$ for IP2 containing random errors are simulated as

$$E = E^{exact} + \text{random}('\text{Normal}', 0, \sigma, I, 1), \tag{54}$$

where $\sigma = \frac{p}{100} \times \max_{x\in\overline{\Omega}} |E^{exact}(x)|$.

In the first two one-dimensional examples we take $t_f = 1$, $k(x) = 1$, $\Omega = (0,1)$, $\omega(t) = 1$, and take $\Delta x = \Delta t = 0.01$ in the FDM for solving the direct, sensitivity and adjoint problems involved in the CGM algorithm.

*4.1. Example 1*

Taking the input data (2), (3), (5) and (6) as

$$S \equiv 0, \quad T_0(x) = (x - x^2)^2 + 20, \quad x \in [0,1], \quad \mu(0,t) = 20e^{-t}, \quad \mu(1,t) = 20e^{-t}, \quad t \in [0,1], \tag{55}$$

$$e(x) = e^{-1}((x - x^2)^2 + 20), \quad x \in (0,1), \quad \text{for IP1}, \tag{56}$$

$$E(x) = (1 - e^{-1})((x - x^2)^2 + 20), \quad x \in (0,1), \quad \text{for IP2}, \tag{57}$$

we obtain the analytical solution, [17],

$$T(x,t) = e^{-t}((x - x^2)^2 + 20), \quad q(x) = \frac{x^4 - 2x^3 + 13x^2 - 12x + 22}{(x - x^2)^2 + 20}. \tag{58}$$

We take the initial guess as $q^0(x) = 1.1$ such that on the boundary $\partial\Omega = \{0,1\}$, the initial guess is equal to the exact solution for $q$ in (58).

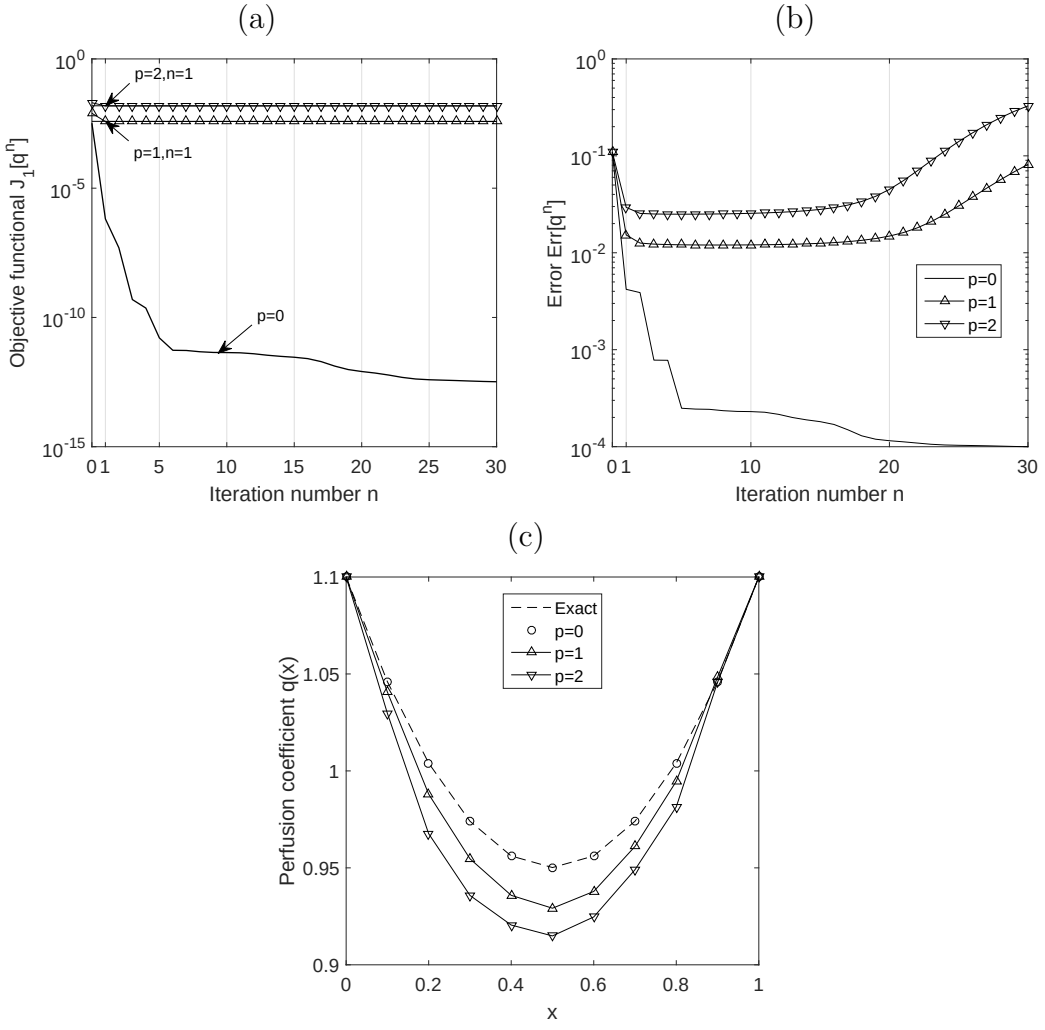


Figure 1: (a) The objective functional (20), (b) the error (52), and (c) the exact and numerical coefficient $q(x)$ for $p \in \{0,1,2\}$ noise, for the IP1 of Example 1.

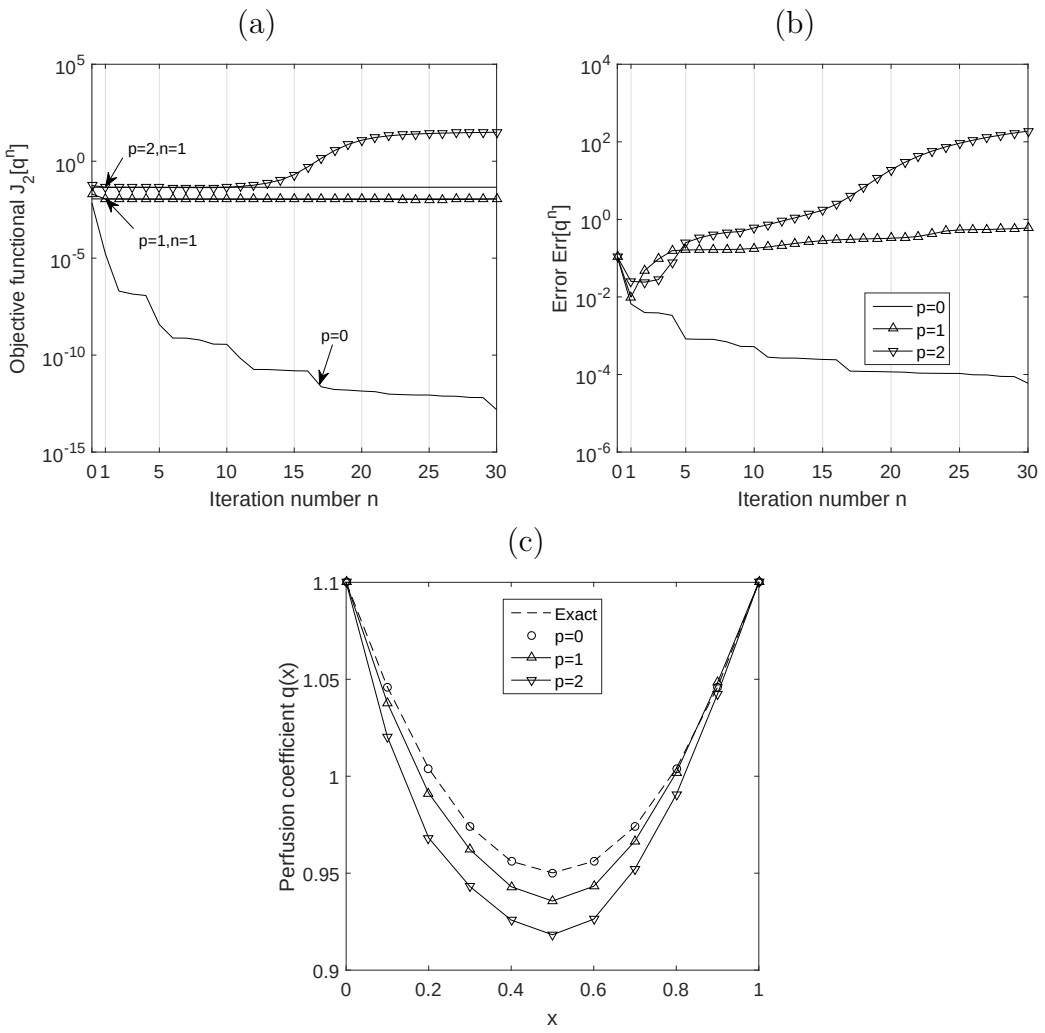


Figure 2: (a) The objective functional (21), (b) the error (52), and (c) the exact and numerical coefficient $q(x)$ for $p \in \{0, 1, 2\}$ noise, for the IP2 of Example 1.

| | Example 1 | | Example 2 | | Example 3 | |
|---|---|---|---|---|---|---|
| $p$ | IP1 | IP2 | IP1 | IP2 | IP1 | IP2 |
| 0 | 1.0E-4 | 5.9E-5 | 0.083 | 0.113 | 0.022 | 0.033 |
| 1 | 1.5E-2 | 9.9E-3 | 0.223 | 0.219 | 0.074 | 0.060 |
| 2 | 2.9E-2 | 2.4E-2 | 0.256 | 0.250 | 0.082 | 0.070 |

Table 1: The error (52) for IP1 and IP2 of Examples 1-3.

Figures 1(a) and 2(a) show the monotonic decreasing convergence of the objective functionals (20) and (21) that are minimized for IP1 and IP2, respectively, as functions of the number of iterations $n$, for various amounts of noise $p \in \{0, 1, 2\}$. For noisy data $p \in \{1, 2\}$, the stopping iteration numbers $n_s \in \{1, 1\}$ are generated according to the discrepancy principle (50). It is clear that the stopping iteration numbers $n_s$ are quite close to the optimal ones in Figures 1(b) and 2(b) which present the error curve (52).

The numerical solutions for IP1 and IP2 are presented in Figures 1(c) and 2(c), respectively. In the case of no noise, the results are plotted after 30 iterations, whilst for noisy data the results are

plotted after $n_s(p) = 1$ iterations. First, it can be seen that in the case of no noise, the retrieved solutions for both IP1 and IP2 are in very good agreement with the exact solution (58). Second, in the case of noisy data, the retrieved solutions are stable and they become more accurate as the amount of noise $p$ decreases. The errors for IP1 and IP2 for various amounts of noise $p \in \{0, 1, 2\}$ are shown in Table 1, and it can be seen that the numerical results for IP2 are more accurate than the numerical results for IP1.

*4.1.1. Comparison with other method*

For Example 1, a comparison for the IP2 can be made with the previous numerical results of [17] obtained by minimizing the first-order Tikhonov regularization functional using the NAG routine E04FCF. In order to keep the numerical simulations as similar as possible the time-average temperature measurement (57) is perturbed by the multiplicative noise

$$E = E^{exact}(1 + \frac{p}{100} \times \eta), \tag{59}$$

where $\eta$ are random variables generated from a uniform distribution in $[-1, 1]$, as in [17], rather than the additive noise (54). In [17], the initial guess was $q^0(x) = 1$, but in our CGM, because of (39) and (41), as the value of $q^n(x)$ remain equal to $q^0(x)$ on $x \in \partial\Omega$, throughout iteration, we take the initial guess as $q^0(x) = 1.1$.

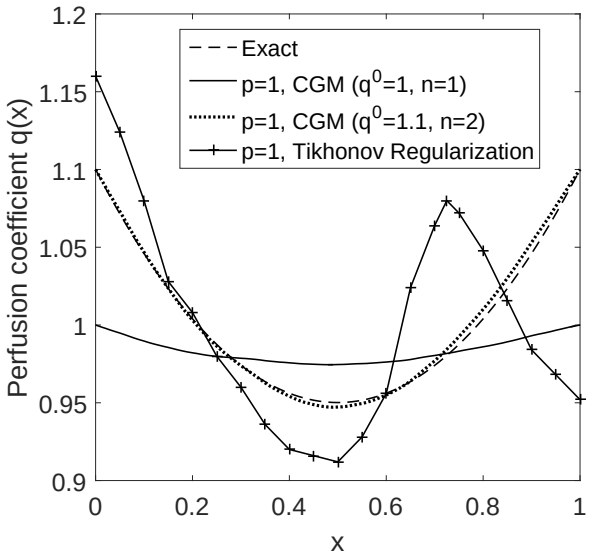


Figure 3: The exact solution (58), the numerical results of [17] (with regularization parameter 0.8 and initial guess $q^0 = 1$), and of the CGM with initial guesses $q^0 = 1$ and $q^0 = 1.1$ for $p\% = 1\%$ noise, for the IP2 of Example 1.

For $p\% = 1\%$ noise in (59), Figure 3 illustrates the comparison between the analytical solution (58), the Tikhonov's regularization numerical results of [17] and those obtained by our CGM with the initial guesses $q^0(x) = 1$ (and stopped after $n = 1$ iteration according to (49)) and $q^0(x) = 1.1$ (and stopped after $n = 2$ iterations according to (49)). From this figure it can be seen that for $p\% = 1\%$ noise in the data (59), both the Tikhonov's regularization of [17] and our CGM under-perform in achieving good agreement with the exact solution (58) when the initial guess is $q^0 = 1$. The CGM over-regularizes the numerical solution when stopped only after $n = 1$ iteration, according to the discrepancy principle (49), whilst the Tikhonov's method

of [17], with the regularization parameter 0.8, under-regularizes the numerical solution, which manifests some unstable oscillations. However, when the initial guess is $q^0 = 1.1$, which ensures that $q^0(x) = q^{exact}(x)$ for $x \in \partial\Omega$, our CGM is very accurate in comparison with the exact solution (58). Unfortunately, we do not have available the numerical results of [17] for the initial guess $q^0 = 1.1$ to compare with. Finally, on comparing Figures 2 and 3 for $p\% = 1\%$ noise and initial guess $q^0 = 1.1$, it can be remarked that the CGM inversion of the data (57) perturbed by the multiplicative noise (59) is more accurate than when the data is perturbed by the additive noise (54).

### *4.2. Example 2*

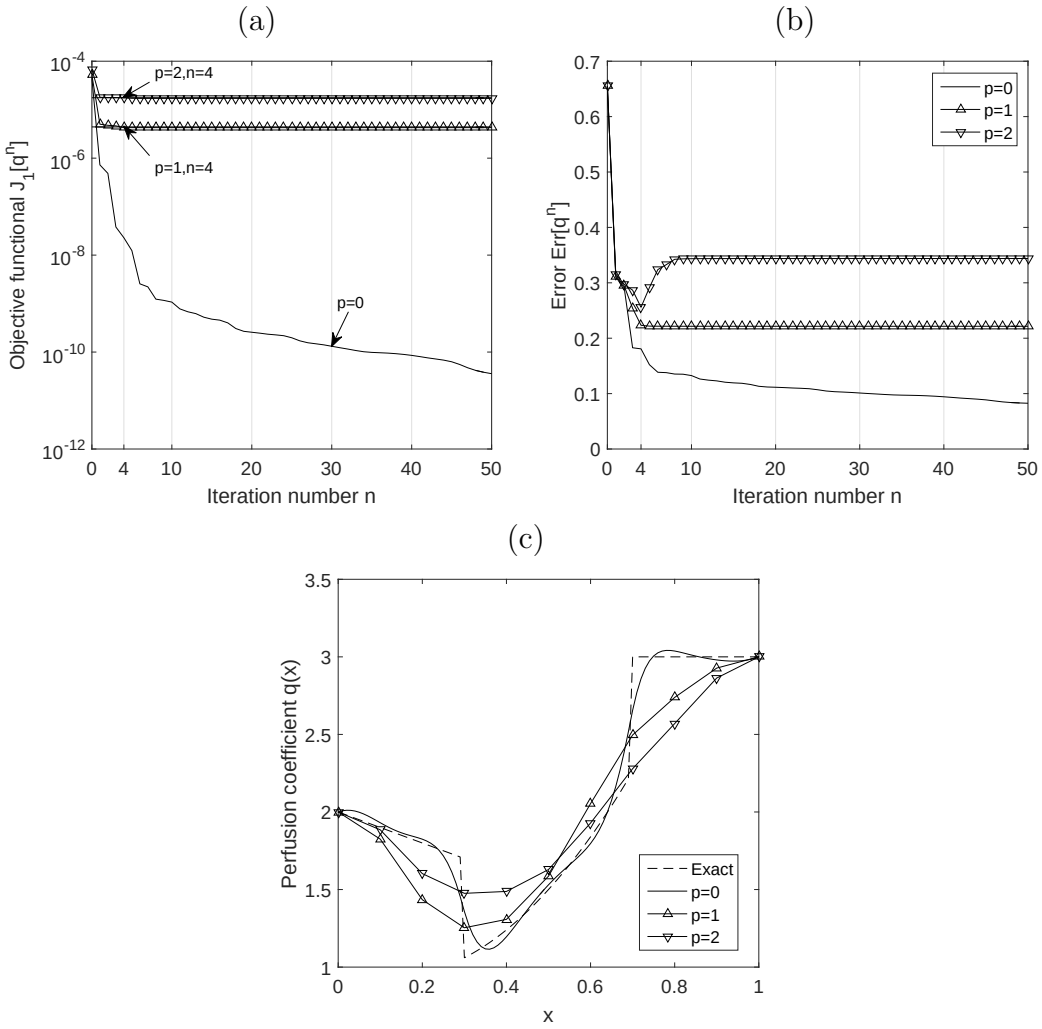


Figure 4: (a) The objective functional (20), (b) the error (52), and (c) the exact and numerical coefficient $q(x)$ for $p \in \{0, 1, 2\}$ noise, for the IP1 of Example 2.

In this example, we take

$$\mu \equiv 0, \quad T_0 \equiv 0, \quad S(x,t) = 2t + x(1-x) + \begin{cases} tx(1-x)(2-x), & x \in [0, 0.3], \\ tx(1-x)(1-x+4x^2), & x \in (0.3, 0.7), \\ 3tx(1-x), & x \in [0.7, 1], \end{cases} \tag{60}$$

$$e(x) = x(1-x), \quad x \in (0,1), \quad \text{for IP1}, \tag{61}$$

$$E(x) = \frac{1}{2}x(1-x), \quad x \in (0,1), \quad \text{for IP2}. \tag{62}$$

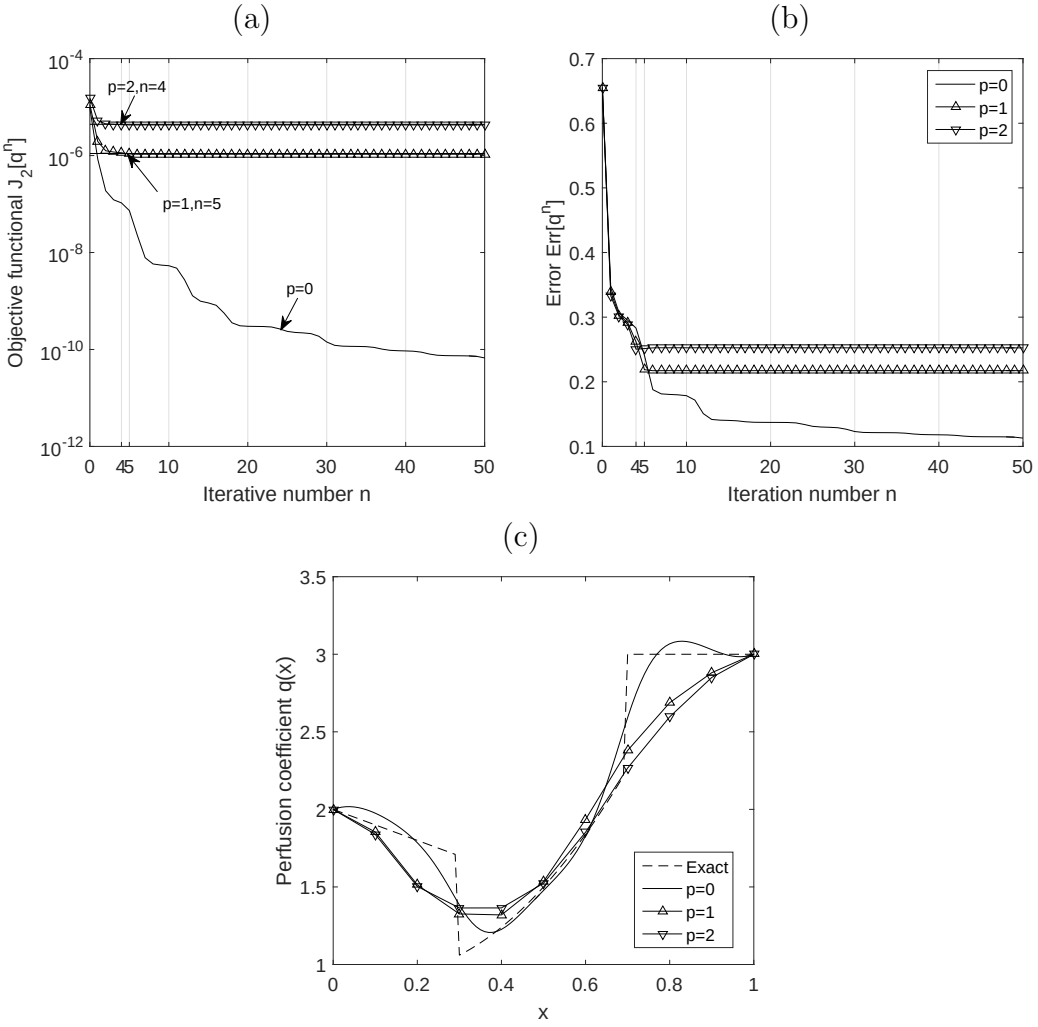


Figure 5: (a) The objective functional (21), (b) the error (52), and (c) the exact and numerical coefficient $q(x)$ for $p \in \{0, 1, 2\}$ noise, for the IP2 of Example 2.

One can observe that the conditions of Theorem 2 are satisfied and hence the solutions of the IP1 and IP2 are unique. In fact it can be verified by direct substitution that the analytical solution is given by

$$T(x,t) = tx(1-x), \quad q(x) = \begin{cases} 2-x, & x \in [0, 0.3], \\ 1-x+4x^2, & x \in (0.3, 0.7), \\ 3, & x \in [0.7, 1]. \end{cases} \tag{63}$$

We take the initial guess as $q^0(x) = x + 2$ which is a linear function passing through the end points $q(0) = 2$ and $q(1) = 3$.

Figures 4(a) and 5(a) show the monotonic decreasing convergence of the objective functionals (20) and (21) that are minimized for IP1 and IP2, respectively. For exact data, i.e. $p = 0$, numerical results are plotted after 50 iterations, while for noisy data $p \in \{1, 2\}$, the stopping iteration numbers generated by the discrepancy principle (50) are $n_s \in \{4, 4\}$ and $n_s \in \{4, 5\}$ for IP1 and IP2, respectively. The error curves (52) are shown in Figures 4(b) and 5(b), and the numerical solutions are presented in Figures 4(c) and 5(c). It is obvious that the numerical results deviate from the exact solution (63) near the discontinuity points $x = 0.3$ and $x = 0.7$. The errors for IP1 and IP2 are shown in Table 1 for $p \in \{0, 1, 2\}$ noise and it can be seen that the errors are quite close to each other for both IP1 and IP2.

*4.3. Example 3*

We consider now a two-dimensional example in the domain $\Omega = (0, 1) \times (0, 1)$, $t_f = 1$ with the input data as

$$\mu \equiv 0, \quad T_0 \equiv 0, \quad k_{11} = k_{22} = 1, \quad k_{12} = k_{21} = 0, \quad \omega \equiv 1, \tag{64}$$

$$S(x, y, t) = (1 + t(1 + x^2 + y^2))xy(1 - x)(1 - y) + t(x(1 - x) + y(1 - y)), \tag{65}$$

$$e(x) = xy(1 - x)(1 - y), \quad (x, y) \in (0, 1) \times (0, 1), \quad \text{for IP1}, \tag{66}$$

$$E(x) = \frac{1}{2}xy(1 - x)(1 - y), \quad (x, y) \in (0, 1) \times (0, 1), \quad \text{for IP2}. \tag{67}$$

One can observe that the conditions of Theorem 2 are satisfied and hence the solutions of the IP1 and IP2 are unique. In fact, it can be verified by direct substitution that the analytical solution is given by

$$T(x, y, t) = txy(1 - x)(1 - y), \quad q(x, y) = 1 + x^2 + y^2. \tag{68}$$

We take $\Delta x = \Delta y = \Delta t = 0.01$ and the initial guess $q^0(x, y) = 1 + x^2 + y^2 + 10xy(1 - x)(1 - y)$ which ensures that $q^0 = q$ on the boundary $\partial\Omega$.

Numerical results and errors presented in Figures 6–9 and Table 1 reveal the same conclusions as those drawn for Examples 1 and 2.

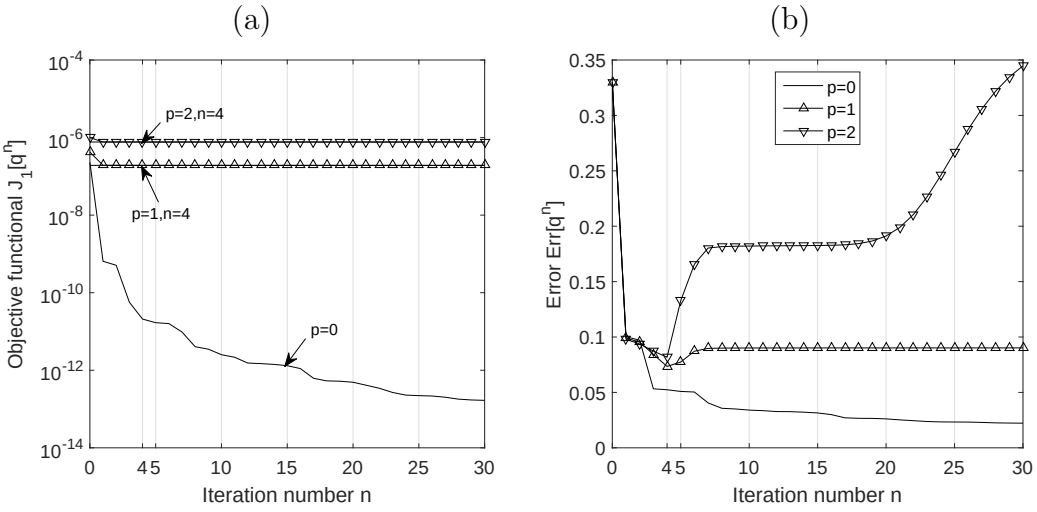


Figure 6: (a) The objective functional (20), (b) the error (52) for $p \in \{0, 1, 2\}$ noise, for the IP1 of Example 3.

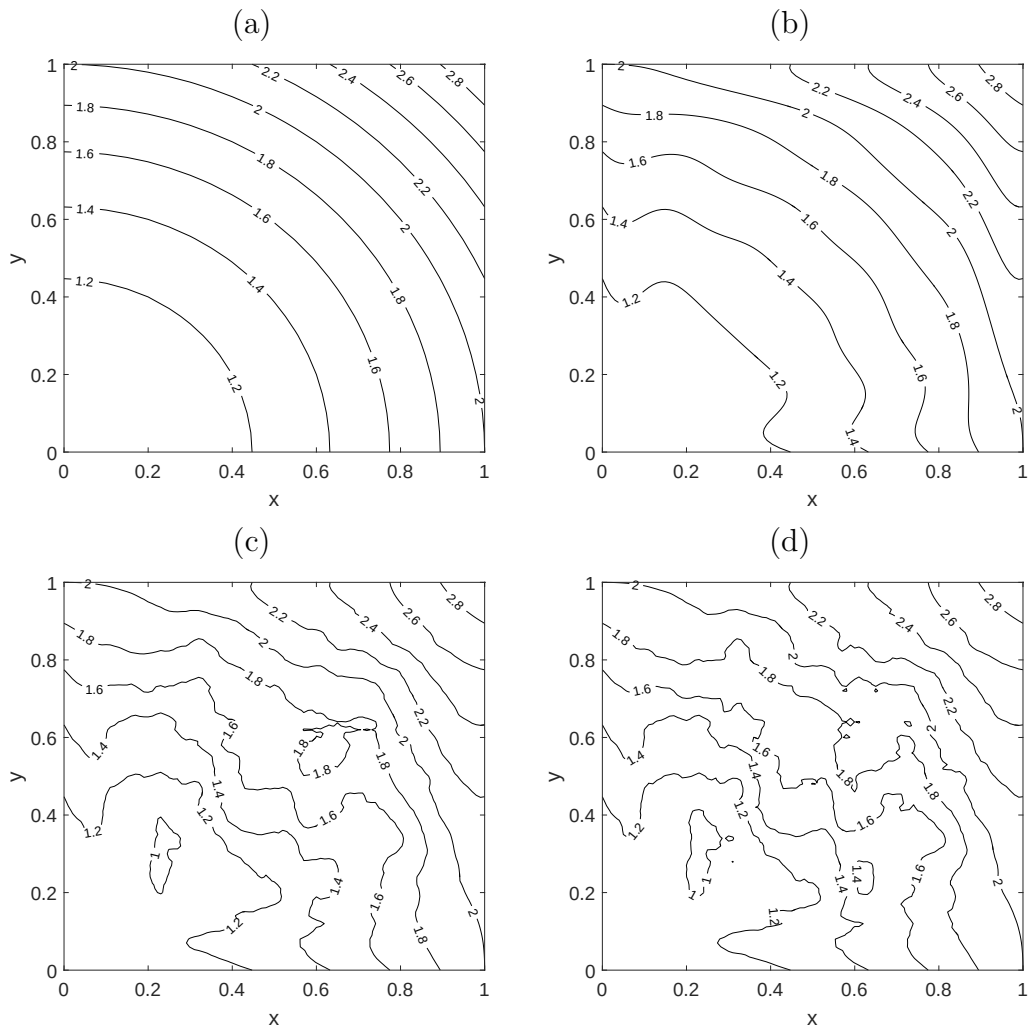


Figure 7: (a) The exact and numerical perfusion coefficient $q(x, y)$ for (b) $p = 0$, (c) $p = 1$ and (d) $p = 2$ noise, for the IP1 of Example 3.

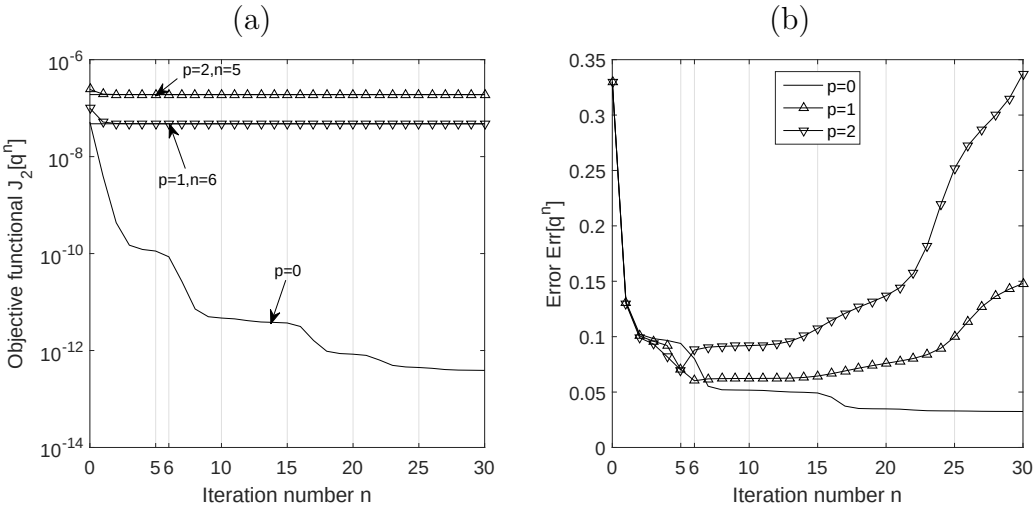


Figure 8: (a) The objective functional (21), (b) the error (52) for $p \in \{0, 1, 2\}$ noise, for the IP2 of Example 3.

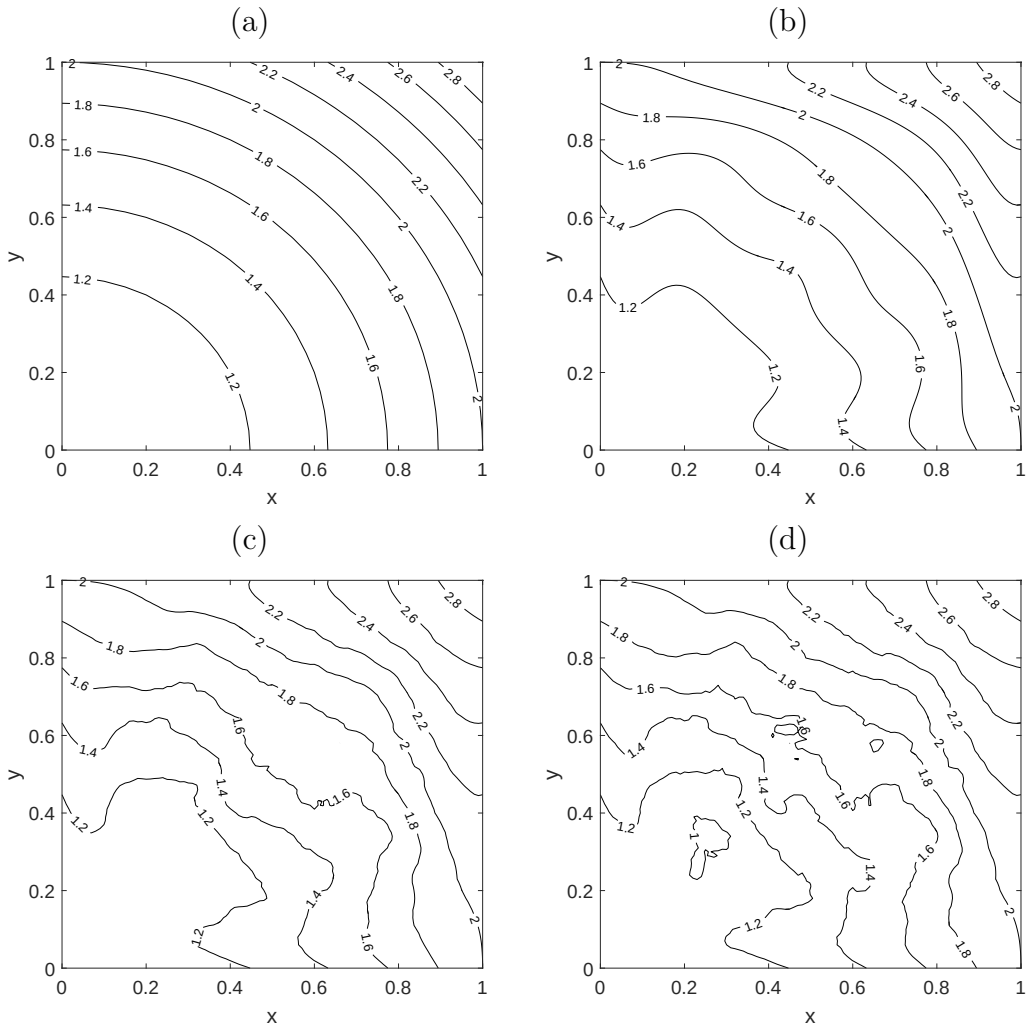


Figure 9: (a) The exact and numerical perfusion coefficient $q(x, y)$ for (b) $p = 0$, (c) $p = 1$ and (d) $p = 2$ noise, for the IP2 of Example 3.

## 5. Conclusions

The numerical CGM analysis developed and verified in this study overcomes the state of the art limits in reconstructing accurately and stably the space-dependent perfusion coefficient from noisy final temperature or time-average temperature measurements. Regularization has been achieved by stopping the iterations at the level at which the least-squares objective functional, minimizing the gap between the computed and the measured data, becomes just below the noise threshold with which the data is contaminated. We have tested three examples for both inverse problems, and found that the numerical solutions are stable and become more accurate as the amount of noise decreases. From Example 2, we also understand that the error becomes larger when the exact perfusion coefficient is discontinuous but still stable and reasonable. The numerical results show that the CGM is an efficient and stable iterative algorithm for reconstructing the perfusion coefficient from minimal data which makes the solution of the inverse problems unique. We have also found out that the numerical solution for the IP2 based on the time-average temperature data (6), which is also more practically realistic, is slightly more accurate than the numerical solution for the IP1 based on the final instant temperature measurement (5). Ultimately, the computational reconstruction undertaken in this study would circumvent reliance on human operators having the

difficult task of measuring accurately the blood's heat capacity and perfusion rate as they vary through the tissue.

**Acknowledgements**

K. Cao would like to thank the University of Leeds and the China Scholarship Council (CSC) for supporting his PhD studies at the University of Leeds.

**References**

[1] P. S. Robinson, E. P. Scott, T. E. Diller, Validation of methodologies for the estimation of blood perfusion using a minimally invasive probe, ASME-Publication-HTD 362 (1998) 109–116.

[2] A. V. Cardinali, T. E. Diller, O. Lanz, E. P. Scott, Validation of a noninvasive thermal perfusion system using a canine medial saphenous fasciocutaneous free tissue flap model, in: ASME 2002 International Mechanical Engineering Congress and Exposition, American Society of Mechanical Engineers, 2002, pp. 9–16.

[3] E. P. Scott, P. S. Robinson, T. E. Diller, Development of methodologies for the estimation of blood perfusion using a minimally invasive thermal probe, Measurement Science and Technology 9 (6) (1998) 888–897.

[4] E. P. Scott, P. S. Robinson, T. E. Diller, Estimation of blood perfusion using a minimally invasive blood perfusion probe, ASME-Publications-HTD 355 (1997) 205–212.

[5] K. Yue, X. Zhang, Y. Y. Zuo, Noninvasive method for simultaneously measuring the thermophysical properties and blood perfusion in cylindrically shaped living tissues, Cell Biochemistry and Biophysics 50 (1) (2008) 41–51.

[6] D. Trucu, D. B. Ingham, D. Lesnic, Inverse time-dependent perfusion coefficient identification, Journal of Physics: Conference Series: 4th AIP International Conference and the 1st Congress of the IPIA 124 (1) (2008) 012050 (28pp).

[7] D. Trucu, D. Ingham, D. Lesnic, Inverse temperature-dependent perfusion coefficient reconstruction, International Journal of Non-Linear Mechanics 45 (5) (2010) 542–549.

[8] W. Rundell, The determination of a parabolic equation from initial and final data, Proceedings of the American Mathematical Society 99 (4) (1987) 637–642.

[9] V. Isakov, Inverse parabolic problems with the final overdetermination, Communications on Pure and Applied Mathematics 44 (2) (1991) 185–209.

[10] A. I. Prilepko, V. V. Solov'ev, Solvability of the inverse boundary-value problem of finding a coefficient of a lower-order derivative in a parabolic equation, Differential Equations 23 (1) (1987) 101–107.

[11] A. I. Kozhanov, A nonlinear loaded parabolic equation and a related inverse problem, Mathematical Notes 76 (5) (2004) 784–795.

[12] V. L. Kamynin, A. B. Kostin, Two inverse problems of finding a coefficient in a parabolic equation, Differential Equations 46 (3) (2010) 375–386.

[13] A. I. Prilepko, A. B. Kostin, On certain inverse problems for parabolic equations with final and integral observation, Russian Academy of Science Siberian Mathematics 75 (1993) 473–490.

[14] L. Yang, J.-N. Yu, Z.-C. Deng, An inverse problem of identifying the coefficient of parabolic equation, Applied Mathematical Modelling 32 (10) (2008) 1984–1995.

[15] Z.-C. Deng, L. Yang, J.-N. Yu, Identifying the radiative coefficient of heat conduction equations from discrete measurement data, Applied Mathematics Letters 22 (4) (2009) 495–500.

[16] Q. Chen, J. Liu, Solving an inverse parabolic problem by optimization from final measurement data, Journal of Computational and Applied Mathematics 193 (1) (2006) 183–203.

[17] D. Trucu, D. B. Ingham, D. Lesnic, Space-dependent perfusion coefficient identification in the transient bio-heat equation, Journal of Engineering Mathematics 67 (4) (2010) 307–315.

[18] O. M. Alifanov, Inverse Heat Transfer Problems, Springer Science & Business Media, Berlin, 2012.

[19] M. N. Ozisik, H. R. B. Orlande, Inverse Heat Transfer: Fundamentals and Applications, CRC Press, Taylor & Francis, New York, 2000.

[20] H. H. Pennes, Analysis of tissue and arterial blood temperatures in the resting human forearm, Journal of Applied Physiology 1 (2) (1948) 93–122.

[21] M. Tadi, M. V. Klibanov, W. Cai, An inversion method for parabolic equations based on quasireversibility, Computers & Mathematics with Applications 43 (8) (2002) 927–941.

[22] D. Trucu, D. B. Ingham, D. Lesnic, Inverse space-dependent perfusion coefficient identification, Journal of Physics: Conference Series 135 (1) (2008) 012098 (8pp).

[23] O. A. Ladyženskaja, V. Solonnikov, N. N. Ural'ceva, Linear and Quasi-linear Equations of Parabolic Type, Vol. 23, American Mathematical Soc., 1988.

[24] A. I. Prilepko, D. G. Orlovsky, I. A. Vasin, Methods for Solving Inverse Problems in Mathematical Physics, CRC Press, New York, 2000.

[25] M. Yamamoto, J. Zou, Simultaneous reconstruction of the initial temperature and heat radiative coefficient, Inverse Problems 17 (4) (2001) 1181–1202.

[26] J. W. Daniel, The Approximate Minimization of Functionals, Prentice-Hall Englewood Cliffs, New Jersey, 1971.

[27] R. Fletcher, C. M. Reeves, Function minimization by conjugate gradients, The Computer Journal 7 (2) (1964) 149–154.

[28] G. I. Marchuk, Methods of Numerical Mathematics, Springer-Verlag, New York, 1975.

[29] S. Islam, S. Ismail, Meshless collocation procedures for time-dependent inverse heat problems, International Journal of Heat and Mass Transfer 113 (2017) 1152–1167.